Experimental and Theoretical Study of a Novel Freeze Desalination System with an Intermediate Cooling Liquid

Reza Kaviani, Hamidreza Shabgard*, Aly Elhefny, Jie Cai, Ramkumar Parthasarathy

School of Aerospace and Mechanical Engineering, University of Oklahoma, Norman, OK 73019, USA

Abstract

Freeze desalination (FD) is a potentially suitable method for treatment of high salinity brines. In this study, a novel FD system utilizing an intermediate cooling liquid (ICL) is fabricated and employed to desalinate brines with salinities up to 100,000 ppm. The FD system consists of a refrigeration unit and a desalination unit that are in thermal communication via the ICL. The desalination unit includes a freezing chamber, several filters, and a centrifugal separator. Feed brine is injected into the cold ICL inside the freezing chamber and partially freezes. The ice is subsequently separated from the ICL and unfrozen concentrated brine. The collected ice contains small amounts of concentrated brine, most of which is drained centrifugally before melting the ice. The developed FD system operates at atmospheric pressure and benefits from the superior heat transfer rates offered by direct contact between the brine and the cooling fluid. Furthermore, it resolves the issues of ice attachment to the cooling surfaces and mixing of refrigerant with the treated water. The effects of the feed brine salinity, cooling temperature, and centrifugation time on the recovery ratio and purity of the treated water were investigated experimentally. Results showed that the recovery ratio increases by decreasing the cooling temperature, and by decreasing the feed brine salinity. However, higher recovery ratios were found to increase the residual salinity in the treated water. For a feed brine with total dissolved solids (TDS) of 70,000 ppm and cooling temperature of -17°C, recovery ratio of about 50% and treated water TDS of ~2600 ppm were achieved experimentally. A theoretical model of the system was also developed and validated against the experimental results.

Keywords: Freeze desalination, Experimental study, High salinity brine, Solid-liquid separation, Intermediate cooling liquid.

Nomenclature

c	specific heat capacity ($\mathrm{kJ/kg \cdot K}$)
EDX	energy dispersive X-ray
FD	freeze desalination
h_{sl}	latent heat of fusion ($\mathrm{kJ/kg}$)
ICL	intermediate cooling liquid
LNG	liquid natural gas
MED	multi-effect desalination
MSF	multi-stage flash
$\dot{m}$	mass flow rate ($\mathrm{kg/s}$)
PDMS	polydimethylsiloxane
$\dot{Q}$	heat transfer rate ($\mathrm{kJ/s}$)
R	recovery ratio, $R = \frac{\dot{m}_{\mathrm{ice}}}{\dot{m}_{\mathrm{fb}}}$
RO	reverse osmosis
S	salinity ($\mathrm{g/kg}$), $S = \frac{m_s}{m_b}$
T	temperature (°C)
TDS	total dissolved solids (ppm)
t	time (minutes)
VFD	variable frequency drive
ρ	density ($\mathrm{kg/m^3}$)
η	desalination rate, $\eta = \frac{m_{s,\mathrm{cb}}}{m_{s,\mathrm{fb}}}$

Subscripts

avg	average
b	brine
cb	concentrated brine
cent	centrifugation
ex	experimental
fb	feed brine
frz	freezing
s	salt
th	theoretical
tw	treated water

1. Introduction

The growing global demand for freshwater and limited resources have resulted in an increasing interest in desalination technologies. Currently, reverse osmosis (RO) and thermal methods, in particular multi-stage flash (MSF) and multi-effect desalination (MED), are the commonly employed large scale desalination technologies. However, all these methods are prone to significant fouling and scaling issues at higher feed brine salinities [1,2].

The freeze desalination (FD) method is a desalination technique that involves cooling the saline water until it partially freezes. Freshwater is extracted in the form of ice, and the remaining unfrozen brine becomes more concentrated [3]. The collected ice contains undesired brine which must be removed before melting the ice. The FD process encounters fewer issues related to scaling, fouling, and corrosion as it operates at low temperatures [4]. From an energy standpoint, the latent heat of fusion of water is almost one-seventh of its latent heat of evaporation, rendering the freezing process inherently less energy intensive than evaporation [4]. The FD method is a suitable candidate for treating the reject brine from the RO processes, thereby approaching zero liquid discharge [5]. Furthermore, FD systems do not require significant pretreatment of the feed, therefore significantly less chemicals are discharged to the environment [1]. Several researchers have studied the application of FD in treatment of oil and gas produced water [6], fruit juice concentration [7], glucose solution concentration [8], dairy products [9], pharmaceutical [10], and wastewater treatment [11].

Freeze desalination can be categorized into direct and indirect contact methods, in terms of brine and refrigerant contact [12,13]. The direct FD method involves using a refrigerant that directly contacts with the saline solution. On the other hand, the indirect FD method employes a thermally conducting solid surface to separate the refrigerant from the saline water. In both direct and indirect FD, the cooling temperature is set below the freezing temperature of the solution [5].

Numerous experimental and numerical [14–17] investigations have been conducted on both direct and indirect contact FD. The indirect FD can be broadly classified into two categories: suspension freeze crystallization and layer freeze crystallization [5]. In suspension freeze crystallization, many small suspended ice crystals are created inside a cooled scraped-surface heat exchanger. The crystals then grow within a stirred growth vessel before proceeding to the separation stage [4]. Layer freeze crystallization results in the formation of an ice crystal layer on top of the cooling surface. Several studies on indirect FD systems have found that as feed brine salinity increases, both the recovery ratio (mass ratio of the produced ice to feed brine) and the desalination rate (ratio of salt mass in the unfrozen concentrated brine to that in the feed brine) decrease [1,18,19]. Furthermore, a reduction in cooling temperature boosts the recovery ratio, while reducing the desalination rate [1]. To lower the salinity of

the produced ice, various quality improvement techniques such as ice pressing [20,21], sweating [22], washing [23], and centrifugation [19,24] are utilized. Desalination rates for indirect FD methods have been reported up to 99% in some experiments [20,24,25]. However, these high desalination rates often correlate with low recovery ratios. Multi-stage FD has also been studied, wherein the treated water is reintroduced into the FD system multiple times to reduce the salinity of the final product [26].

One of the early studies on direct FD was done by Landau and Martindale [27] who experimentally studied the effect of various operational parameters on the ice quality. Their results showed that lowering the feed brine salinity and refrigerant flow rate resulted in a higher quality of the produced ice. The spray freezing of seawater by utilizing a process where Freon-114 and saltwater feed were sprayed through nozzles was studied by Gibson et al [28]. To separate the residual Freon from the ice crystals, a pressurized wash column was employed. Their findings highlighted the importance of maintaining sufficient turbulence to prevent the formation of an ice-cake layer near the nozzles. The continuous brine crystallization using butane as the refrigerant was carried out by Wiegandt et al. [29]. Their findings showed that atomizing the liquid creates a substantial heat transfer area and promotes strong turbulent flows, facilitating an efficient heat transfer process. More recently, Xie et al. [30] developed a FD setup in which cold energy from LNG was used to cool down another liquid which was mixed with the seawater. They used HFE-7100 as the intermediate cooling liquid and injected it inside a cylinder filled with seawater and collected the formed ice. Their findings showed that with lowering the refrigerant temperature, the ice generation rate increased while the desalination rate decreased. The HFE-7100 used by Xie et al. as the intermediate cooling liquid has a relatively high vapor pressure at room temperature (26.9 kPa) which can potentially lead to the loss of the cooling liquid due to evaporation. It is also prohibitively expensive and has a relatively small specific heat [31,32].

In general, it can be deduced from the available literature that the primary benefit of indirect FD is the refrigerant-free treated water with potentially improved quality. This is attributed to the relatively slow and controlled freezing process which reduces the likelihood of brine entrapment between ice crystals [5]. On the other hand, direct FD methods benefit from higher ice production rate due to enhanced heat transfer between the refrigerant and the saline water [2]. The specific power consumption is also lower in direct contact FD compared to the indirect FD [5]. The primary drawback of indirect FD is its relatively higher energy consumption, stemming from the reduced heat transfer rate between the refrigerant and the feed brine, as well as design complexities due to scrapping of the ice from the cooled surfaces [13]. On the other hand, the primary challenges associated with direct freeze desalination include the presence of residual refrigerant in the treated water and the difficulty in controlling the freezing process, both of which degrade the quality of the treated water [33]. Another challenge shared

by both direct and indirect FD methods is separating the residual brine from the ice before melting it. The residual brine dissolves in the melted ice and increases the salinity of the treated water [4].

Considering the existing research on FD technologies and the proposed designs available in the literature, there is a lack of FD systems that can effectively combine the desired features of both direct and indirect FD systems while minimizing their drawbacks. Such a hybrid FD system can potentially lead to more promising solutions for desalination of high concentration brines and pave the way for their large-scale deployment.

In the present work, we attempt to fill this research gap by developing an FD system that bridges direct and indirect methods. In this design, the cooling fluid and the brine are directly mixed. However, unlike the conventional direct FD where the refrigerant fluid of the refrigeration cycle is mixed with the brine, we employ an intermediate cooling liquid which circulates between a refrigeration unit and a desalination unit. The employed cooling liquid in this study is silicon oil. Compared to previously used liquids, the silicone oil offers significant advantages including no volatility at room temperature, greater specific heat, and substantially lower price [32,34,35]. Besides, the developed FD system incorporates an integrated ice crushing technique that reduces brine entrapment and enhances the desalination rate. The primary objective of this work is to establish the proof of concept for a novel FD system utilizing an intermediate cooling liquid to address the inherent challenges associated with traditional FD systems.

The rest of the manuscript is organized as follows: Section 2 describes the experimental setup. The thermodynamic analysis of the freezing process of the brine and related energy transfer are presented in Sec. 3. Finally, in Sec. 4 the results of various experiments focusing on the impact of the most influential operation parameters are presented and discussed.

2. Experimental setup

An experimental setup is fabricated to study the performance of the proposed novel FD system with an intermediate cooling liquid (ICL) [36]. Figure 1 shows the actual and schematic views of the fabricated FD system. It is composed of a desalination unit and a refrigeration unit, that are coupled via the ICL. The ICL is a silicone fluid and recirculates between the evaporator section of the refrigeration unit and the desalination unit. The desalination unit is consisted of the following sections: a freezing chamber in which the feed brine is injected into and mixed with the cold ICL, a filter bag separator which separates the ice crystals from the rest of the slurry, a second filter separator for separation of the unfrozen concentrated brine from the ICL, and a slurry transport section through which the slurry/ICL circulates. In the following, further details on each of these sections are provided. The component numbers referenced in the following sections are with respect to Fig. 1b.

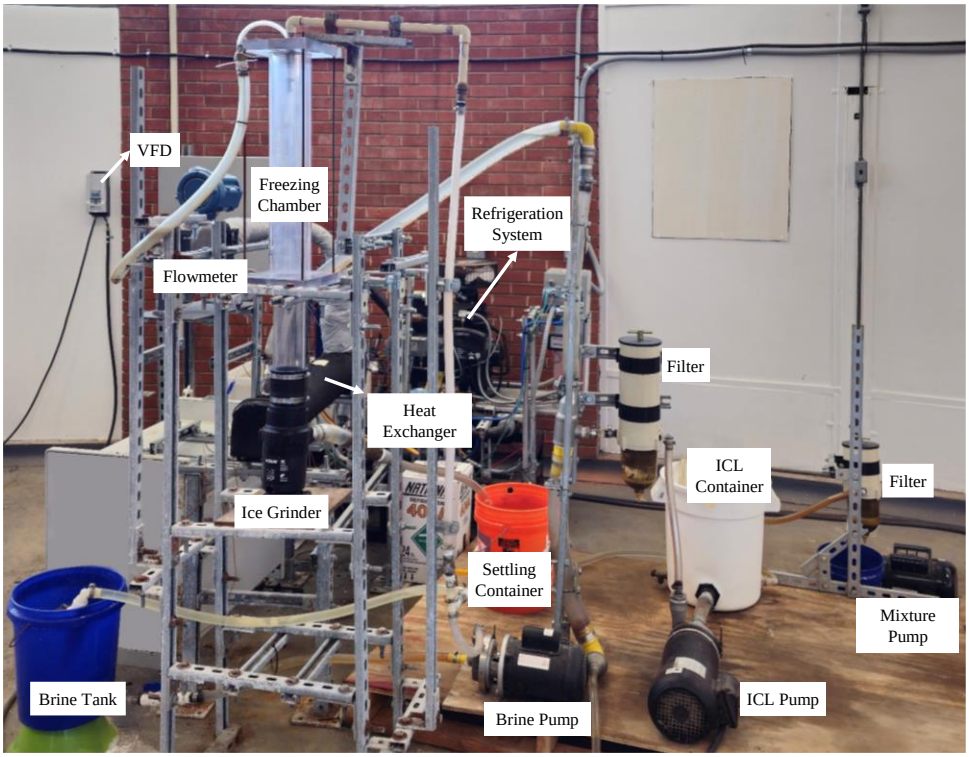

(a)

(b)

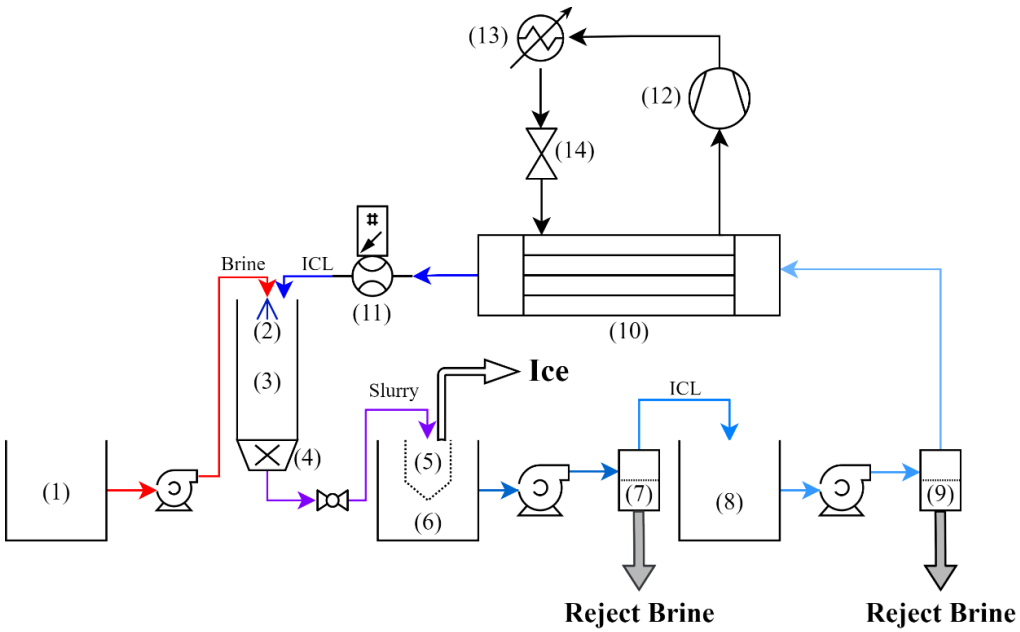

Fig. 1 (a) Experimental setup and (b) the schematic view of it. Description of the components in the schematic view: (1) brine tank, (2) brine spray nozzle, (3) freezing chamber, (4) ice grinder, (5) ice-liquid separation filter bag, (6) settling tank, (7) first brine-ICL separation filter, (8) ICL tank, (9) second brine-ICL separation filter, (10) heat exchanger, (11) flowmeter, (12) compressor, (13) condenser, (14) expansion valve.

Refrigeration system

The ICL is cooled by a refrigeration unit operating with R-404A refrigerant. The refrigeration unit consists of a compressor (12), condenser (13), expansion valve (14), and evaporator (10). The compressor is a three-phase reciprocating compressor, Copelametic HFC-404A, with nominal power of 2.44 kW at a saturated evaporating temperature of -31.7°C. A horizontal shell-and-tube heat exchanger, shown in Fig. 2, serves as the evaporator compartment of the refrigeration unit. The shell and the tubes are made of steel and copper, respectively. The heat exchanger is 0.91 m long and has an internal diameter of 0.127 m, providing a maximum heat transfer rate of 42 kW. The refrigerant R-404A and the ICL flow in the tube side and shell side of the heat exchanger, respectively, in a counterflow arrangement. The outer surface of the heat exchanger was insulated by a layer of insulation foam with a thickness of 3 cm. The cooling capacity of the refrigeration system was controlled by modulating the electronic expansion valve opening through a LabVIEW graphical user interface to achieve the desired cooling temperature. The refrigerant flow rate and temperature at the inlet and outlet of the evaporator and condenser were recorded during the operation. The condenser of the refrigeration system consists of a 4.5 m copper tube with an inner diameter of 0.011 m, which was formed into a coil and submerged in a water tank.

Fig. 2 The shell-and-tube heat exchanger and the ICL and refrigerant (R404-A) inlets and outlets

Brine preparation and injection

Brine with various salinities was prepared by adding regular table salt to tap water (tap water TDS ≈ 250 ppm). The elemental composition of the table salt was analyzed using energy dispersive X-ray (EDX) method and the results are presented in table 1. As evident, sodium chloride constitutes nearly 96% of the salt mass. Salt was added to water gradually and the solution was thoroughly mixed. The TDS of the resulting feed brine was measured using a Hanna Instruments HI2300 TDS meter and additional salt was added until the desired TDS was achieved. The feed brine temperature and flow rate during the tests were maintained constant at 20°C and 0.13 kg/min, respectively. The brine was pumped from the brine tank (1) by a stainless-steel corrosion-resistant centrifugal pump and was injected into

the cold ICL through a nozzle (2) as small droplets in the range of 50 μm to 100 μm. The small size of brine particles improves the heat transfer by increasing the contact surface area between the brine and the cold ICL.

Table 1. The EDX analysis of the salt

Component	Weight percentage
C	2.6 %
O	1.4 %
Na	37.4 %
Cl	58.5 %
Mo	0.1 %

Crystallization and slurry separation

The ICL from tank 8 (see Fig. 1) was pumped to the shell side of the shell-and-tube heat exchanger. The ICL flow rate was controlled by a three-phase low-temperature stainless-steel corrosion-resistant pump driven by a variable frequency drive (VFD). The mass flow rate of the ICL was measured by an Emerson Micro Motion Coriolis mass flow meter (11) with an accuracy of ±0.1% of the reading, installed downstream of the heat exchanger. The freezing chamber (3) was made from a 1-meter long polycarbonate cylindrical tube with an inner diameter of 10 cm and a wall thickness of 0.5 cm. A second polycarbonate cylindrical tube with a height of 70 cm and an inner diameter of 12 cm was placed around the upper section of the inner cylinder and the annular space between the two cylinders was vacuumed. The double wall design around the upper section of the freezing chamber prevented condensation on the outer surface of the freezing chamber, thereby improving visual access to the freezing process and decreasing the heat gain. The cold ICL at a constant flow rate and temperature entered the freezing chamber from the top. Brine was injected from the top of the freezing chamber as well and ice crystals formed inside. To avoid ice agglomeration and clogging, a rotary ice grinder device (4) was placed at the bottom of the freezing chamber to crush the chunks of ice. The ice grinder also improved the mixing and heat transfer between the brine droplets and the ICL by creating a swirling motion inside the freezing chamber. A short video showing the ice formation in the freezing chamber is provided as a supplementary material. The ice crystals, unfrozen concentrated brine, and ICL exiting the ice grinder were transferred through a hose to the ice-liquid separation filter bag (5). The filter separated the ice from the liquid mixture of concentrated brine and ICL.

The separated ice contained small amounts of concentrated brine and ICL and is referred to as “wet ice” in what follows. The liquid mixture passing through the filter bag was pumped to the first oil-water separation filter (7). The flow rate of the liquid out of the settling tank (6) was controlled by adjusting the pump speed

using a variable voltage transformer. The oil-water filter separator trapped the brine and let the ICL pass through. The separated brine was collected at the bottom of the filter and was gradually discharged through a discharge valve at the bottom of the separator. The dewatered ICL was passed to the main ICL tank (8). To assure a complete ICL-brine separation, a second oil-water separation filter (9) was placed before the heat exchanger.

The ICL is a PDMS (Polydimethylsiloxane) silicone fluid sold under various names by different companies. In this work, the silicone fluid was purchased from "Clearco Products" company under the commercial name "PSF-1.5 cSt Silicone Fluid". Thermophysical properties of the ICL are presented in table 2 [34]. As can be seen, this fluid has a low freezing temperature and low viscosity at low temperatures, and a low vapor pressure at room temperature. Furthermore, it is non-toxic and immiscible with water. Compared to alternative immiscible cooling liquids with low freezing temperature and viscosity, specifically the HFE-7100 and similar liquids from the 3M™ Novec™ family, the selected silicone oil offers some important advantages: Silicone oil has a vapor pressure of 0.13 kPa at 25°C, making it non-volatile at room temperature. In contrast, HFE-7100 has a vapor pressure of 26.9 kPa at 25°C which makes it more volatile under the same conditions. The silicone fluid also has a greater specific heat than HFE-7100 and similar 3M™ Novec™ fluids. Quantitatively, the specific heat of PSF-1.5 cSt silicone fluid is 1715 J/kg·K at 25°C versus 1183 J/kg·K for HFE-7100 [31]. Furthermore, the price per kg of silicone fluid is significantly less than that of 3M™ Novec™ fluids [32,35,37].

Table 2. Thermophysical properties of silicone liquid (ICL) [34]

Freezing point	-70°C
Specific gravity at 25°C	0.851
Specific heat capacity at 25°C	1,715 J/kg·K
Viscosity at 25°C	1.5 cSt
Viscosity at -25°C	3 cSt
Vapor pressure 25°C	0.13 kPa

Centrifugal separation

As the feed brine freezes partially inside the freezing chamber, the concentration of the unfrozen brine increases since the salt is repelled from the ice crystals. Some of this brine adheres to the surface of the ice crystals or is trapped inside them. Thus, the ice-brine separation step is a crucial part of the freeze desalination process to achieve low salinity treated water. We employed a centrifugal method to separate the concentrated brine and residual ICL from the collected wet ice. The wet ice was centrifuged by a spin-dryer spinning at 3200 rpm for 4 to 16 minutes. Most of the liquid was rejected by centrifugation and the drained ice contained significantly less liquid. The collected liquid contains both ICL and unfrozen

concentrated brine. The ICL can be effectively separated from unfrozen brine through gravitational separation since the unfrozen brine density is 30% to 35% greater than the ICL. The gravitational separation is further facilitated by the immiscibility of ICL and brine, as well as its low viscosity. Finally, the drained ice was collected and melted, and its TDS was measured. Since the recovery ratio and the salinity of the treated water were found to be dependent on the duration of the centrifugation, various centrifugation times were tested and compared, which will be discussed in Sec. 4.4.

3. Theoretical analysis and performance metrics

By spraying the feed brine into the cold ICL, the temperature of the brine droplets decreases until the freezing temperature corresponding to the TDS of the feed brine is reached. The phase diagram of a basic binary salt-water solution is shown in Fig. 3. Considering point "A" as the initial condition of the feed brine, cooling of the brine does not affect its salinity until the temperature reaches the ice line at point "B" (also known as the liquidus line). Further cooling of the solution results in partial removal of water from the solution in the form of ice and increasing salinity of the unfrozen brine along the ice line. As the temperature decreases, both the amount of ice and the salinity of the remaining brine increase. Further cooling of the solution brings the solution to the eutectic point "C" [38]. At temperatures lower than the eutectic point, the salt-hydrate and ice form simultaneously and no liquid is remained [5].

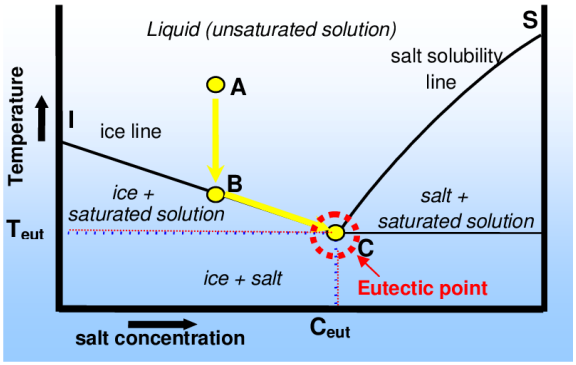

Fig. 3 Phase diagram of a binary salt-water solution [39]

The mass fraction of the generated ice upon cooling can be determined theoretically using an energy balance applied to the freezing chamber. Figure 4 depicts the inlet and outlet streams of the freezing chamber. The inputs to the freezing chamber are the feed brine and cold ICL, and the output streams are ice, unfrozen concentrated brine, and ICL.

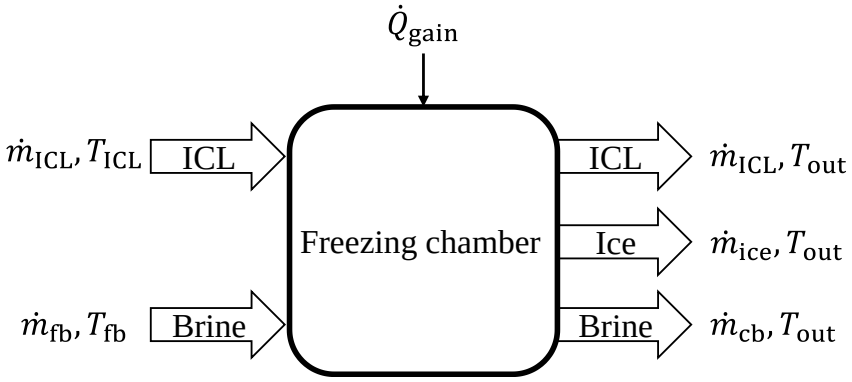

Fig. 4 Freezing chamber inlet and outlet streams

The following assumptions are considered:

1. The mixture in the freezing chamber is well mixed and all components, namely, ice, unfrozen concentrated brine, and ICL leave the freezing chamber at the same temperature.
2. The specific heat and density of the ICL are constant.
3. The salt is pure sodium chloride.

The energy balance for the freezing chamber is as follows:

$$\dot{m}_{\text{ICL}} c_{\text{ICL}} (T_{\text{out}} - T_{\text{ICL}}) = \dot{m}_{\text{fb}}\, c_{\text{avg}} (T_{\text{fb}} - T_{\text{out}}) + \dot{m}_{\text{ice}} h_{\text{sl}} + \dot{Q}_{\text{gain}} \quad (1)$$

where $\dot{m}_{\text{ICL}}$, $\dot{m}_{\text{fb}}$, and $\dot{m}_{\text{ice}}$ are the mass flow rates of ICL, feed brine, and generated ice, respectively, c_{ICL} and c_{avg} are the specific heat of the ICL, and the mass-averaged specific heat of the ice-brine mixture, respectively, and h_{sl} is the latent heat of fusion of ice. Also, in Eq. (1), T_{ICL}, T_{fb}, and T_{out} are the temperature of the inlet ICL, the feed brine, and the outlet mixture, respectively, and $\dot{Q}_{\text{gain}}$ is the heat gain from the ambient to the freezing chamber due to imperfect insulation.

The mass-averaged specific heat of the ice-brine mixture is defined as:

$$c_{\text{avg}} = \frac{\dot{m}_{\text{fb}}\, c_{\text{fb}} + \dot{m}_{\text{ice}}\, c_{\text{ice}} + (\dot{m}_{\text{fb}} - \dot{m}_{\text{ice}}) c_{\text{cb}}}{2\, \dot{m}_{\text{fb}}} \quad (2)$$

where c_{fb}, c_{ice}, and c_{cb} are the specific heat of the feed brine, produced ice, and concentrated brine, respectively.

The recovery ratio is defined as the mass flow rate of the produced ice to that of the feed brine:

$$R = \frac{\dot{m}_{\mathrm{ice}}}{\dot{m}_{\mathrm{fb}}} \tag{3}$$

Equations (1) and (2) can be rewritten using the recovery ratio as:

$$\dot{m}_{\mathrm{ICL}} c_{\mathrm{ICL}} (T_{\mathrm{out}} - T_{\mathrm{ICL}}) = \dot{m}_{\mathrm{fb}} \left[c_{\mathrm{avg}} (T_{\mathrm{fb}} - T_{\mathrm{out}}) + R h_{\mathrm{sl}} \right] + \dot{Q}_{\mathrm{gain}} \tag{4}$$

$$c_{\mathrm{avg}} = \frac{1}{2} [c_{\mathrm{fb}} + R\, c_{\mathrm{ice}} + (1 - R) c_{\mathrm{cb}}] \tag{5}$$

As a result of crystallization, the concentration of the unfrozen brine increases gradually through the freezing chamber. As such, the thermophysical properties of the concentrated brine including density, specific heat, latent heat of fusion, and freezing temperature vary from the inlet to the outlet. The variations of these properties as a function of the brine salinity can be described by the equations presented in table 3 [40–42], where S denotes the salinity in grams of salts per kilogram of the brine, $S = m_s/m_b$ (g/kg). It is noted that these properties are derived for aqueous sodium chloride, however, since sodium chloride constitutes about 96% of the salt used in this study these equations can be adopted with acceptable accuracy.

Table 3. Thermophysical properties of aqueous sodium chloride as a function of salinity S (g/kg) [40–42]

Property	**Equation**
Density (kg/m^3)	$\rho_b = S + 997$
Specific heat capacity (kJ/kg · K)	$c_b = -0.0007232\, S + 4.178$
Latent heat of fusion (kJ/kg)	$h_{\mathrm{sl}} = -0.0003\, S^2 - 0.074\, S + 333$
Freezing temperature (°C)	$T_{\mathrm{frz}} = -0.0002\, S^2 - 0.043\, S$

The efficiency of freeze desalination is often characterized by a metric named desalination rate, defined as the mass of salt in the rejected unfrozen concentrated brine to the mass of salt in the feed brine [17,30,43,44]:

$$\eta = \frac{m_{s,\mathrm{cb}}}{m_{s,\mathrm{fb}}} = 1 - R \left(\frac{S_{\mathrm{ice}}}{S_{\mathrm{fb}}} \right) \tag{6}$$

where $m_{s,\mathrm{cb}}$ and $m_{s,\mathrm{fb}}$ are the mass of salt in the unfrozen concentrated brine and feed brine, and S_{ice} and S_{fb} are the salinities of the melted produced ice and feed brine, respectively. Since we measured the TDS instead of salinity in the present work, the desalination rate should be rewritten in terms of TDS. For a solution in which all the dissolved solids are salts salinity and TDS are related by $S_{\mathrm{b}} = \mathrm{TDS}_b/\rho_b$. Since in the present work salts constitute about 96% of the dissolved mass the same

conversion between salinity and TDS can be applied. The desalination rate in terms of TDS can be written as:

$$\eta = 1 - R\left(\frac{\rho_{\mathrm{fb}}}{\rho_{\mathrm{ice}}}\right)\left(\frac{\mathrm{TDS}_{\mathrm{ice}}}{\mathrm{TDS}_{\mathrm{fb}}}\right) \tag{7}$$

Using the first equation in table 3, the density of the brine can be expressed in terms of its TDS as $\rho_b = 498.5 + \sqrt{498.5^2 + \mathrm{TDS}_{\mathrm{b}}}$. Substituting this expression in Eq. (7), the desalination rate at any recovery ratio can be obtained from the measured TDS values of the ice and feed brine. The outlet temperature of the freezing chamber corresponds to the freezing temperature of the concentrated brine at the outlet, which in turn is a function of the salinity of the concentrated brine, S_{cb}. The salinity of the concentrated brine can be obtained as a function of the feed brine salinity, desalination rate, and recovery ratio:

$$S_{\mathrm{cb}} = \eta\frac{S_{\mathrm{fb}}}{1 - R} \tag{8}$$

The outlet temperature (in °C) as a function of the salinity of the concentrated brine (in g of salt per kg of brine) can be obtained using the fourth equation in table 3.

Equations (6) to (8) and those shown in table 3 are based on salinity. The heat gain during the freezing process was determined experimentally. To do so, the ICL was circulated through the system without brine injection at the same flow rate and temperature as the system with brine injection. After the steady state was reached, the temperature difference of the ICL across the freezing chamber was measured and was used to calculate the heat gain:

$$\dot{Q}_{\mathrm{gain}} = \dot{m}_{\mathrm{ICL}}c_{\mathrm{ICL}}\left(T_{\mathrm{ICL,out}} - T_{\mathrm{ICL}}\right) \tag{9}$$

where $T_{\mathrm{ICL,out}}$ is the ICL temperature exiting the freezing chamber without brine injection. The temperature rise of the ICL was measured to be about 1°C for an ICL flow rate of 5 kg/min.

Having the heat gain determined, for any given T_{ICL}, $\dot{m}_{\mathrm{ICL}}$, T_{fb}, $\dot{m}_{\mathrm{fb}}$, and S_{fb}, the recovery ratio, R, the outlet temperature, T_{out}, and the salinity of the concentrated brine, S_{cb}, can be calculated from Eqs. (4), (5), (8), and those presented in table 3, as a function of desalination rate (η). The desalination rate is obtained from the measurement of the treated water TDS after the centrifugation process for each experiment individually.

4. Results & discussion

The primary goal of freeze desalination is creating a low salinity water stream from the feed brine while maintaining a reasonable recovery ratio. Both objectives are affected by multiple parameters, most notably the cooling temperature, feed brine salinity, and ice-brine separation efficacy. This section begins with studying the effect of cooling temperature on the recovery ratio and quality of the produced ice. Next, the feed brine salinity effect is studied, followed by the effect of centrifugation time. It is noted that in all the tests reported here, the outlet temperature of the freezing chamber was always higher than the threshold temperature for formation of salt-hydrates. Therefore, salt-hydrates did not form and the only solid substance in the system was ice.

The experimental uncertainties were assessed by considering random (precision) error, the least count of instruments, and their respective accuracies. To address random error, each experiment was conducted three times, and the average value of the pertinent parameter was used for presentation and calculations. The measuring devices — the scale, flowmeter, and TDS meter — have least counts of 0.01 g, 0.0001 kg/s, and 100 ppm, respectively. The accuracies of these instruments are ±1%, ±0.1%, and ±1% of the reading, respectively. Experimental results had uncertainties ranging from 6% to 10% for TDS, 3% to 6% for R, and 0.1% to 2% for η.

4.1. Cooling temperature effect

One of the critical factors affecting the recovery ratio and water quality is the cooling temperature of the brine. In this section, the effect of this temperature on the recovery ratio and quality of the treated water is studied at a fixed feed brine TDS of 70,000 ppm and an ICL mass flow rate of 5 kg/min. The feed brine flow rate and temperature were also fixed at 0.13 kg/min and 20°C, respectively. Four cooling temperatures (the temperature at the outlet of the freezing chamber) of -10°C, -14°C, -17°C, and -20°C were tested. These temperatures were achieved by controlling the inlet ICL temperatures through adjusting the cooling power provided by the refrigerant. The steady ICL flow and brine injections were established, and the cooling power was adjusted until the desired temperature at the outlet of the freezing chamber was achieved. The collected ice was centrifuged by the spin-dryer for 12 minutes to drain the liquids. The spin-dryer was placed inside a freezer to retain the ice temperature below the melting point during centrifugation. The freezer temperature was maintained at around -10°C. The drained ice was recovered from the spin-dryer and its mass and TDS were measured after melting. Samples of the drained ice are shown in Fig. 5.

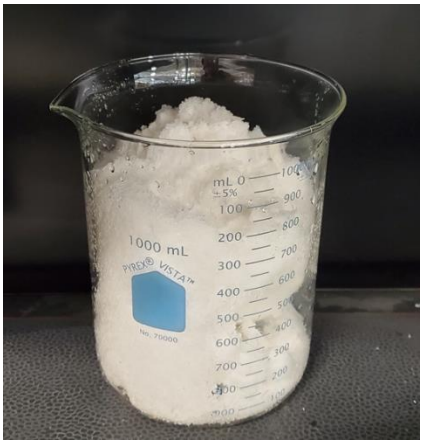

Fig. 5 Produced ice after centrifugal draining

The effect of the cooling temperature on the recovery ratio and TDS of the drained ice after melting (treated water) is shown in Fig. 6 for a centrifugation time of 12 minutes. As expected, lowering the cooling temperature results in higher recovery ratios. The TDS of the treated water (TDS_{tw}) was 3300, 2700, 2200, and 1800 ppm for the cooling temperatures of -20°C, -17°C, -14°C, and -10°C, respectively. The lower TDS of the treated water at relatively higher cooling temperatures can be attributed to the slower ice crystallization, which provides more time for the ice crystals to repel the brine. Conversely, at lower cooling temperatures, crystallization occurs faster, resulting in a greater amount of brine entrapment within the ice. The inverse relationship between the TDS of the treated water in FD systems and the temperature of the freezing process has been reported by several investigators [19,20,45,46]. Another reason for the lower TDS of the treated water at relatively high cooling temperatures might be the lower mass ratio of ice to unfrozen brine. The lower ice formation results in a smaller rise in the salinity of the unfrozen brine. Thus, the unfrozen brine entrapped in the ice also has a lower TDS. It can be concluded that there is a tradeoff between the recovery ratio and TDS of the treated water.

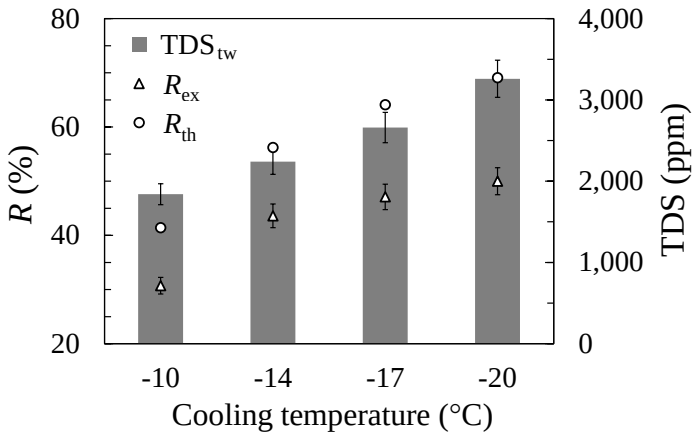

Fig. 6 Theoretical (R_{th}) and experimental (R_{ex}) recovery ratios and corresponding TDS of the treated water (TDS_{tw}) for feed brine TDS of 70,000 ppm and various cooling temperatures. The error bars represent the overall uncertainty of the measurements.

Figure 6 also shows the theoretically determined recovery ratios at various cooling temperatures. As evident, the theoretical results overpredict the recovery ratios compared to the experimental data. This is potentially due to partial melting and loss of ice inside the filter bag and during transportation to the spin-dryer device and centrifugation.

4.2. Brine salinity effect

Another influential factor that can significantly affect the recovery ratio and salinity of the treated water is the feed brine salinity. Lower brine salinities are expected to lead to lower salinity of the produced ice. However, as will be shown, the cooling temperature and recovery ratio can influence the salinity of the produced ice beyond the feed salinity. In this section, the experimentally determined recovery ratios and treated water TDS at four feed brine salinities of 15,000 ppm, 35,000 ppm, 70,000 ppm, and 100,000 ppm and a cooling temperature of -17°C are presented and compared. The ICL and feed brine flow rates were 5 kg/min and 0.13 kg/min, respectively, and the feed brine inlet temperature was 20°C. The collected ice was separated from the concentrated brine by 12 minutes of centrifugation.

Figure 7 shows the experimental and theoretical recovery ratios and treated water TDS for multiple feed brine salinities. As expected, the recovery ratio decreased by increasing the feed brine TDS. However, interestingly the salinity of the produced ice was lower for higher feed brine TDS. This seemingly counterintuitive result can be attributed to the rate of freezing. At a fixed cooling temperature and feed brine flow rate, lowering the feed brine salinity results in greater amount of ice generation during the same period of time, which corresponds to a higher rate of ice crystallization. The faster crystallization rates increase the likelihood of concentrated brine entrapment within the ice crystals. These small pockets of entrapped brine are hard to remove by centrifugal draining, and if left inside the ice increase the TDS of the treated water upon melting of the ice. The effect of faster freezing rates on the higher salinity of treated water has also been reported in previous studies [1,30,44].

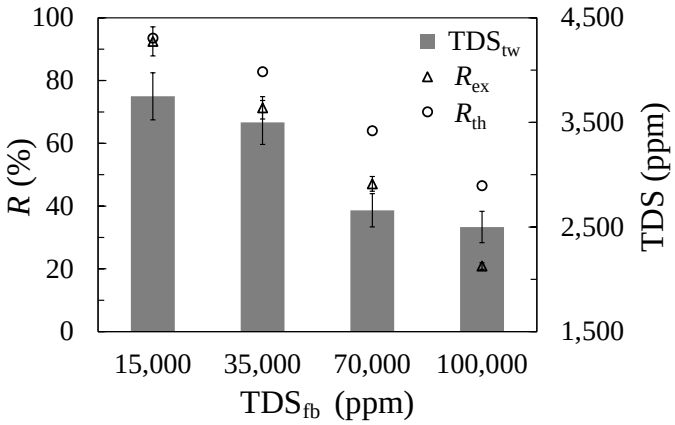

Fig. 7 Theoretical (R_{th}) and experimental (R_{ex}) recovery ratios and corresponding TDS of the treated water (TDS_{tw}) for cooling temperature of -17°C and various feed brine salinities (TDS_{fb}). The error bars represent the overall uncertainty of the measurements.

Both experimentally and theoretically determined recovery ratios decrease by increasing the feed brine TDS. It can be observed in Fig. 7 that at lower feed TDS levels, the experimental results for recovery ratio are closer to the theoretical ones, but their deviation grows as the feed salinity increases. The poor agreement at higher feed brine TDS levels can be attributed to the greater amount of unintended ice melting during transport and centrifugation of ice. For higher brine TDS, the entrapped brine within the ice also has higher TDS. The ice adjacent to these high salinity brine pockets is more likely to melt during the centrifugation.

Figure 8 shows the experimentally determined desalination rates, η, and the associated recovery ratios, R_{ex}, for various feed salinities and a cooling temperature of -17°C. It is evident that for a fixed cooling temperature increasing the feed brine salinity improves the desalination rate and decreases the recovery ratio.

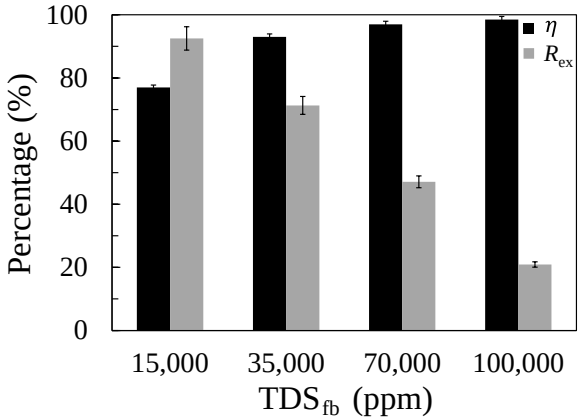

Fig. 8 Experimentally determined desalination rate (η) and recovery ratio (R_{ex}) for a cooling temperature of -17°C and multiple feed brine salinities (TDS_{fb}). The error bars represent the overall uncertainty of the measurements.

4.3. The effect of the duration of the centrifugal brine removal

As previously discussed, the collected ice contains brine that needs to be removed effectively before melting the ice. A portion of the unfrozen brine adheres to the surface of ice crystals, while another fraction is trapped within them. To remove the brine from the ice, a centrifugal method was employed. The centrifugation time was found to affect the recovery ratio and the quality of the treated water. Various centrifugation durations (t_{cent}) from 4 to 16 minutes were investigated. Table 4 presents the recovery ratio, TDS of the treated water, and the desalination rate for various centrifugation times for a feed brine TDS of 70,000 ppm and a cooling temperature of -17°C. The high desalination rate indicates that a noticeable amount of unfrozen brine was present within the ice prior to centrifugation. Further increase of the centrifugation time did not affect the TDS significantly. It is noted that the efficacy of the centrifugal separation improves by utilizing devices with higher rpm. This adjustment results in shorter separation time and can reduce energy consumption of the separation process.

Table 4. The experimental recovery ratio (R_{ex}) and TDS of the treated water (TDS_{tw}) and desalination rate (η) for a feed brine TDS of 70,000 ppm and cooling temperature of -17°C for various centrifugation durations (t_{cent}).

t_{cent} (minutes)	R_{ex} (%)	TDS_{tw}(ppm)	η (%)
4	53.1	7,370	93.4
8	48.5	4,650	96.3
12	47.1	2,660	97.9
16	45.8	2,100	98.6

Figure 9 shows the variations of the recovery ratio and treated water TDS with the centrifugation duration. As evident, increasing the centrifugation time results in smaller TDS_{tw} and recovery ratios. Increasing the brine removal from the ice by a longer centrifugation time has two simultaneous effects: on one hand, it diminishes the amount of unfrozen brine within the ice, and as such decreases the total mass of the ice recovered from the spin-dryer which translates into a smaller recovery ratio. On the other hand, the TDS of the treated water improves because there is less unfrozen brine in the recovered ice. The desalination rate for centrifugation times of 4, 8, 12, and 16 minutes are about 93%, 96%, 98%, and 99%, respectively. Notably, the desalination rate improves by about 3% by increasing the centrifugation time from 4 minutes to 8 minutes, while increasing it from 12 minutes to 16 minutes improves the desalination rate by about

1%. The lessened enhancement in the desalination rate can be ascribed to the difficulty in brine rejection at later times when the ice becomes "drier" and the remaining brine becomes harder to expel. Consequently, for centrifugation times longer than ~16 minutes, the brine rejection becomes negligible and only slight variations in recovery ratio and TDS of the treated water occur.

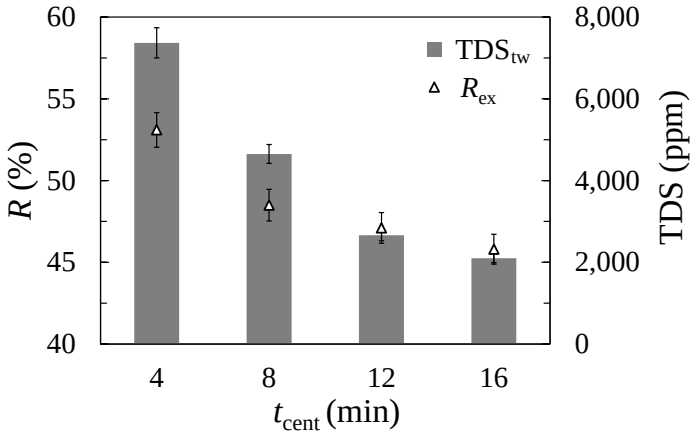

Fig. 9 Experimental recovery ratio (R_{ex}) and corresponding TDS of the treated water (TDS_{tw}) for feed brine TDS_{fb} of 70,000 ppm and cooling temperature of -17°C. The error bars represent the overall uncertainty of the measurements.

5. Conclusions

In this study, a novel freeze desalination system with an intermediate cooling liquid was fabricated and tested for treatment of high salinity brine. Experiments were conducted to measure the recovery ratio and the TDS of the treated water for different cooling temperatures, feed brine salinities, and centrifugation times. The following main conclusions were drawn:

- The experimental results showed that at constant feed brine salinity, as the cooling temperature decreased the recovery ratio increased. However, the TDS of the treated water was higher at lower cooling temperatures. This can be ascribed to the faster crystallization rates at lower cooling temperatures, which results in less time for salt rejection and higher salt entrapment within the ice crystals.
- The experimental findings demonstrated that at a fixed cooling temperature, the ice generation was greater for feed brine with smaller salinities. However, the salinity of the treated water was lower for feed brines with greater salinities. This can also be explained by the faster crystallization at lower feed brine TDS.
- Longer centrifugation times resulted in better removal of unfrozen concentrated brine from the ice, leading to lower TDS of the treated water. However, the recovery ratio diminished due to

the decreased mass of the recovered ice. Centrifugation times greater than ~16 minutes had negligible effect on recovery ratio and salinity of the treated water.

Acknowledgement

Support from the Advanced Research Projects Agency-Energy (ARPA-E) under Award Number DE-AR0001069 is acknowledged and appreciated.

References

[1] S. Moharramzadeh, S.K. Ong, J. Alleman, K.S. Cetin, Parametric study of the progressive freeze concentration for desalination, Desalination. 510 (2021) 115077. https://doi.org/10.1016/j.desal.2021.115077.

[2] B. Kalista, H. Shin, J. Cho, A. Jang, Current development and future prospect review of freeze desalination, Desalination. 447 (2018) 167–181. https://doi.org/10.1016/j.desal.2018.09.009.

[3] P.M. Williams, M. Ahmad, B.S. Connolly, D.L. Oatley-Radcliffe, Technology for freeze concentration in the desalination industry, Desalination. 356 (2015) 314–327. https://doi.org/10.1016/j.desal.2014.10.023.

[4] A. Najim, A review of advances in freeze desalination and future prospects, Npj Clean Water. 5 (2022). https://doi.org/10.1038/s41545-022-00158-1.

[5] I. Janajreh, H. Zhang, K. El Kadi, N. Ghaffour, Freeze desalination : Current research development and future prospects, Water Res. 229 (2023) 119389. https://doi.org/10.1016/j.watres.2022.119389.

[6] E.T. Igunnu, G.Z. Chen, Produced water treatment technologies, Int. J. Low-Carbon Technol. 9 (2014) 157–177. https://doi.org/10.1093/ijlct/cts049.

[7] Z. Ding, F.G.F. Qin, J. Yuan, S. Huang, R. Jiang, Y. Shao, Concentration of apple juice with an intelligent freeze concentrator, J. Food Eng. 256 (2019) 61–72. https://doi.org/10.1016/j.jfoodeng.2019.03.018.

[8] S. Samsuri, N.A. Amran, M. Jusoh, Spiral finned crystallizer for progressive freeze concentration process, Chem. Eng. Res. Des. 104 (2015) 280–286. https://doi.org/10.1016/j.cherd.2015.06.040.

[9] H. Jaster, G.D. Arend, K. Rezzadori, V.C. Chaves, F.H. Reginatto, J.C.C. Petrus, Enhancement of antioxidant activity and physicochemical properties of yogurt enriched with concentrated strawberry pulp obtained by block freeze concentration, Food Res. Int. 104 (2018) 119–125. https://doi.org/10.1016/j.foodres.2017.10.006.

[10] D. Weber, J. Hubbuch, Raman spectroscopy as a process analytical technology to investigate biopharmaceutical freeze concentration processes, Biotechnol. Bioeng. 118 (2021) 4708–4719. https://doi.org/10.1002/bit.27936.

[11] S. Samsuri, N.A.N. Rizan, S.H. Hung, N.A. Amran, N.S. Sambudi, Progressive freeze concentration for volume reduction of produced water and biodiesel wastewater, Chem. Eng. Technol. 42 (2019) 1764–1770. https://doi.org/10.1002/ceat.201800505.

[12] K.S. Spiegler, A.D.K. Laird, eds., Principles of desalination (Part B), Elsevier, 2012.

[13] M.S. Rahman, M. Ahmed, X.D. Chen, Freezing-melting process and desalination: I. review of the state-of-the-art, Sep. Purif. Rev. 35 (2006) 59–96. https://doi.org/10.1080/15422110600671734.

[14] C.W. Ong, C.L. Chen, Technical and economic evaluation of seawater freezing desalination using liquefied natural gas, Energy. 181 (2019) 429–439. https://doi.org/10.1016/j.energy.2019.05.193.

[15] Y. Liu, T. Ming, Y. Wu, R. De Richter, Y. Fang, N. Zhou, Desalination of seawater by spray freezing in a natural draft tower, Desalination. 496 (2020) 114700. https://doi.org/10.1016/j.desal.2020.114700.

[16] H. Jayakody, R. Al-Dadah, S. Mahmoud, Numerical investigation of indirect freeze desalination using an ice maker machine, Energy Convers. Manag. 168 (2018) 407–420. https://doi.org/10.1016/j.enconman.2018.05.010.

[17] A. Eghtesad, M. Salakhi, H. Afshin, S.K. Hannani, Numerical investigation and optimization of indirect freeze desalination, Desalination. 481 (2020) 114378. https://doi.org/10.1016/j.desal.2020.114378.

[18] P. Sahu, S. Krishnaswamy, N.K. Pande, Process intensification using a novel continuous U-shaped crystallizer for freeze desalination, Chem. Eng. Process. - Process Intensif. 153 (2020) 107970. https://doi.org/10.1016/j.cep.2020.107970.

[19] D. Chen, C. Zhang, H. Rong, C. Wei, S. Gou, Experimental study on seawater desalination through supercooled water dynamic ice making, Desalination. 476 (2020) 114233. https://doi.org/10.1016/j.desal.2019.114233.

[20] L. Erlbeck, D. Wössner, K. Schlachter, T. Kunz, F. Methner, M. Rädle, Investigation of a novel scraped surface crystallizer with included ice- pressing section as new purification technology, Sep. Purif. Technol. 228 (2019) 115748. https://doi.org/10.1016/j.seppur.2019.115748.

[21] L. Erlbeck, M. Rädle, R. Nessel, F. Illner, W. Müller, K. Rudolph, T. Kunz, F.J. Methner,

Investigation of the depletion of ions through freeze desalination, Desalination. 407 (2017) 93–102. https://doi.org/10.1016/j.desal.2016.12.009.

[22] Y. Mandri, A. Rich, D. Mangin, S. Abderafi, C. Bebon, N. Semlali, J.P. Klein, T. Bounahmidi, A. Bouhaouss, Parametric study of the sweating step in the seawater desalination process by indirect freezing, Desalination. 269 (2011) 142–147. https://doi.org/10.1016/j.desal.2010.10.053.

[23] J. Chang, J. Zuo, K.J. Lu, T.S. Chung, Freeze desalination of seawater using LNG cold energy, Water Res. 102 (2016) 282–293. https://doi.org/10.1016/j.watres.2016.06.046.

[24] H. Yang, M. Fu, Z. Zhan, R. Wang, Y. Jiang, Study on combined freezing-based desalination processes with microwave treatment, Desalination. 475 (2020) 114201. https://doi.org/10.1016/j.desal.2019.114201.

[25] M. Hasan, N. Rotich, M. John, M. Louhi-Kultanen, Salt recovery from wastewater by air-cooled eutectic freeze crystallization, Chem. Eng. J. 326 (2017) 192–200. https://doi.org/10.1016/j.cej.2017.05.136.

[26] A. Alkhalidi, S. Kiwan, A. Al-Hayajneh, Experimental investigation of water desalination using freezing technology, Case Stud. Therm. Eng. 28 (2021) 101685. https://doi.org/10.1016/j.csite.2021.101685.

[27] M. Landau, A. Martindale, Assessment of crystalliser designs for a butane freeze desalination process, Desalination. 3 (1967) 318–329. https://doi.org/10.1016/S0011-9164(00)80161-7.

[28] W. Gibson, D. Emmermann, G. Grossman, R. Johnson, A. Modica, A. Pallone, Spray freezer and pressurized counterwasher for freeze desalination, Desalination. 14 (1974) 249–262. https://doi.org/10.1016/S0011-9164(00)80258-1.

[29] H.F. Wiegandt, A. Madani, P. Harriott, Ice crystallization developments for the butane direct-contact process, Desalination. 67 (1987) 107–126. https://doi.org/https://doi.org/10.1016/0011-9164(87)90237-2.

[30] C. Xie, L. Zhang, Y. Liu, Q. Lv, G. Ruan, S.S. Hosseini, A direct contact type ice generator for seawater freezing desalination using LNG cold energy, Desalination. 435 (2018) 293–300. https://doi.org/10.1016/j.desal.2017.04.002.

[31] Heat transfer applications using 3M ™ Novec ™ engineered fluids, 2013. https://multimedia.3m.com/mws/media/1091997O/3m-novec-engineered-fluids-for-heat-transfer-line-card.pdf.

[32] Silmid, (2023) https://www.silmid.com/us/specialties/specialty-ch.

[33] M. Shafipour Rahman, M. Al-khusaibi, Freezing-melting desalination process, in: Desalin. Water from Water, 2014: pp. 473–501.

[34] PSF - 1.5 cSt silicone heat transfer fluid product information, 2023. https://doi.org/https://www.clearcoproducts.com/pdf/volatile/NP-PSF-1_5cSt.pdf.

[35] Gelest, (2023) https://www.gelest.com/product/DMS-T01.5/.

[36] H. Shabgard, R.N. Parthasarathy, J. Cai, Zero liquid discharge eutectic freeze desalination with intermediate cold liquid, U.S. Patent Application No. 17/095,675, 2021. https://patents.google.com/patent/US20210139346A1/en.

[37] P. Gorbounov, M. Battistin, E. Thomas, Comparison of liquid coolants suitable for single-phase detector cooling, (2016) 1–17.

[38] B. Verbeek, Eutectic freeze crystallization on sodium chloride - analysis of a full experimental cycle, Msc. Thesis, Technical University of Delf, 2011. http://resolver.tudelft.nl/uuid:2d3bca49-1f4f-41f1-a2aa-b821712d82ec.

[39] F.E. Genceli, Scaling-up eutectic freeze crystallization, PhD Thesis, Technical University of Delf, 2008. http://resolver.tudelft.nl/uuid:c64d84d8-6552-4d3c-9c02-1d511c689c43.

[40] M.M. Conde, M. Rovere, P. Gallo, Molecular dynamics simulations of freezing-point depression of TIP4P/2005 water in solution with NaCl, J. Mol. Liq. 261 (2018) 513–519. https://doi.org/10.1016/j.molliq.2018.03.126.

[41] H. Kumano, T. Asaoka, A. Saito, S. Okawa, Formulation of the latent heat of fusion of ice in aqueous solution, Int. J. Refrig. 32 (2009) 175–182. https://doi.org/10.1016/j.ijrefrig.2008.07.010.

[42] H. Zhang, I. Janajreh, M.I. Hassan Ali, K. Askar, Freezing desalination: Heat and mass validated modeling and experimental parametric analyses, Case Stud. Therm. Eng. 26 (2021) 101189. https://doi.org/10.1016/j.csite.2021.101189.

[43] A. Zambrano, Y. Ruiz, E. Hernández, M. Raventós, F.L. Moreno, Freeze desalination by the integration of falling film and block freeze-concentration techniques, Desalination. 436 (2018) 56–62. https://doi.org/10.1016/j.desal.2018.02.015.

[44] C.S. Luo, W.W. Chen, W.F. Han, Experimental study on factors affecting the quality of ice crystal during the freezing concentration for the brackish water, Desalination. 260 (2010) 231–238. https://doi.org/10.1016/j.desal.2010.04.018.

[45] W. Lin, M. Huang, A. Gu, A seawater freeze desalination prototype system utilizing LNG cold energy, Int. J. Hydrogen Energy. 42 (2017) 18691–18698.

https://doi.org/10.1016/j.ijhydene.2017.04.176.

[46] H.M. Abdelmoaty, A.U. Mahgoub, A.W. Abdeldayem, Performance analysis of salt reduction levels in indirect freeze desalination system with and without magnetic field exposure, Desalination. 508 (2021) 115021. https://doi.org/10.1016/j.desal.2021.115021.